A Comprehensive Experimental Investigation of Tubular Entry Flow of Viscoelastic Fluids:

Part III. Unstable Flow

P. J. CABLE

Department of Chemical Engineering
Monash University
Clayton, Victoria, Australia

and
D. V. BOGER

Department of Chemical Engineering
University of Delaware
Newark, Delaware 19711

For every viscoelastic fluid studied in the contraction geometry, it was found that increasing the flow rate beyond a certain limit resulted in disturbance to the stable entry flow patterns described in Parts I and II. An examination of the development of the entry flow disturbances was carried out using still and cine photography. Still photographs are presented to illustrate the characteristics of the unstable flow patterns. The time varying nature of the flow has been recorded on a cine film *Flow Patterns in Abrupt Entry Flow of Viscoelastic Fluids* which is available for loan. Critical condition criteria for the onset of the periodic flow disturbances were obtained in terms of the fundamental fluid properties and are presented and compared with other suggested criteria for the onset of unstable entry flow of viscoelastic fluids.

PERIODIC ENTRY FLOW DISTURBANCES

It has been shown in Parts I and II that two stable flow regimes exist in laminar entry flow of viscoelastic fluids, namely, the vortex growth regime at low flow rates and divergent flow at moderate flow rates. While the vortex growth regime was characterized by unique entry flow patterns, it was possible in the 4:1 contraction to maintain an entirely different, unsteady entry flow pattern at the same flow rates for which divergent flow was observed. That is, beyond the flow rate at which the maximum in vortex size occurred, there were two different entry flow patterns which could be obtained at exactly the same conditions of flow rate, pressure, and temperature. If the flow rate were slowly increased from the vortex growth regime, a steady, two-dimensional flow pattern was observed, divergent flow (Figure 8 in Part I). On the other hand, if the flow rate were initially very high, with random distortions occurring in the entry flow, and the flow was then throttled back to the same condition as that for divergent flow, a periodic three-dimensional flow was obtained. Both the flow patterns were seen to persist for several hours, well beyond any possible transient or fluid memory effect.

Divergent flow could only be obtained by increasing the flow rate from an initial condition in the vortex growth regime and not by decreasing the flow from a state of periodic or random distortion. That is, decreasing the flow rate yields an abrupt transition from periodic flow to the vortex growth regime. This leads to the conclusion that the divergent flow is a metastable condition. In Part II, the occurrence of concavities in the axial velocity profiles in the divergent flow was demonstrated. The effect of such concavities on the stability of flow was discussed. It is not unreasonable to conclude that the divergent flow is metastable and that the periodic disturbances constitute the preferred entry flow configuration.

The nature of the periodic flow is illustrated in Figure 1 for fluid F9 in the 4:1 contraction. Three still photographs, taken a short time interval apart, are shown. The flow conditions for these photographs were identical to those for which the divergent flow pattern in Figure 8*b* in Part I was obtained; that is, $N'_{Re} = 165$, $N_{WS} = 0.635$. The flow is undergoing a spiralling or swirling disturbance. Viewed in two dimensions, as in Figure 1, the converging fluid stream whips up and down like a wave on an elastic string, while the two sections of the vortex, at the top and bottom of the tube, alternately increase and decrease in size. The frequency of the distortion is quite regular. It should be stressed that the fluid particles themselves do not spiral into the small tube as along a corkscrew. Rather, there is an asymmetric distortion to the streamlines which rotates around the tube center line with a regular frequency. The extremes of this asymmetric distortion are shown in the right- and left-hand frames of Figure 1. The spiralling flow is three dimensional, and it is difficult to visualize such a flow from two-dimensional cross-sectional views. This is in contrast to the divergent flow obtained at the same conditions, which has no azimuthal component, and the velocity varies only in the axial and radial directions. The regular nature of the spiralling distortions is well illustrated on the cine film.

Correspondence concerning this paper should be addressed to D. V. Boger, Monash University, Clayton, Victoria, Australia. P. J. Cable is with ICI Limited, Ascot Vale, Victoria, Australia.

Part I of this paper appeared in the *AIChE J.*, 24, 869 (1978).
Part II appeared in the *AIChE J.*, 24, 992 (1978).

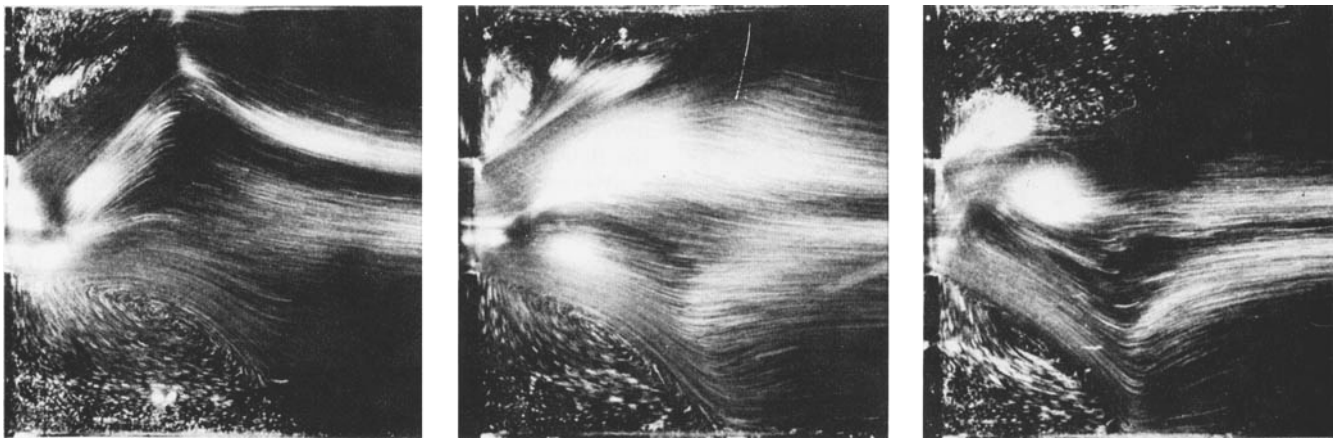

Fig. 1. Flow patterns upstream of the 4:1 contraction for fluid F9 at 350 cm³/s, showing spiralling flow ($N_{Re}' = 165$, $N_{WS} = 0.635$, 1/25 s at f/5.6). (Sequence 1-3 taken short time interval apart.)

The frequency of the spiralling flow increased with increasing flow rate. The frequency was measured by timing a number of the cyclic flow perturbations. Figure 2 shows the variation of the frequency (ω) with flow rate for four fluids (V2, F3, F5, F6) in the 4:1 contraction. The range of downstream wall shear rates corresponding to the flow rates was $590 < \dot{\gamma}_w < 2\,500\ s^{-1}$. Figure 3 shows the variation of $\omega\theta$ with N'_{Re}, where θ is the Maxwell relaxation time of the fluid estimated at the downstream wall shear rate. The product $\omega\theta$ is essentially constant for each fluid in the intermediate N'_{Re} range (approximately $100 < N'_{Re} < 300$). Deviations at the higher shear rates may be due to inaccuracies introduced by the extrapolation of fluid property measurements.

The maximum value of N'_{Re} in Figure 3 is 410, which corresponds to a generalized Reynolds number of 1 310:

$$N'_{Re} = \rho \frac{D^n V^{2-n}}{K} \tag{1}$$

$$N_{Re,\,gen} = \rho \frac{D^n V^{2-n}}{K} \cdot 8^{1-n} \left(\frac{4n}{3n+1} \right) \tag{2}$$

Criteria for turbulence in generalized Newtonian fluids may be framed in terms of the generalized Reynolds number exceeding 2 000 to 2 500 (Metzner and Reed, 1955). Thus, it is clear that the flow in the downstream tube is laminar for all cases where spiralling flow was observed.

Dual steady flow states were observed at flow rates above that for maximum vortex size for almost all fluids studied in the 4:1 contraction. The exceptions were F4 and F13, which both showed significantly smaller values for the stress ratio than the remainder of the test fluids. While this observation in itself is not sufficient to explain the absence of spiralling flow for these two fluids, it may be an indication that there were significant differences in other fluid properties which were not measured, perhaps second normal stress difference and/or extensional viscosity. Fluids F4 and F13 correlated well with the vortex size data of the other fluids but represented the extreme deviations.

Over a limited range of flow rates in the dual flow regime, it was found that a third steady flow pattern could also be obtained for fluids V1, V2, F5, and F14. Figures 4, 5, and 6 show the three different entry flow patterns in the 4:1 contraction for fluid F14 at a flow rate of 154 cm³/s, for which $N'_{Re} = 127$ and $N_{WS} = 0.493$. In Figure 4, the steady two-dimensional divergent flow pattern is illustrated. The vortex size is identical at the top and bottom of the tube and does not vary with time. The spiralling flow, which can occur at the same flow rate, is shown in Figure 5. Two extremes of the flow pattern distortion are pictured, with the top and bottom sections of the vortex alternately collapsed to minimum size or fully extended upstream. The asymmetric distortion to the converging streamlines, which causes them to whip up and down when viewed in two dimensions, moves circumferentially around the tube center line with a regular frequency.

The third flow pattern, which was obtained at the identical flow rate to that for the other two, is illustrated by four still photographs in Figure 6. The flow is pulsing

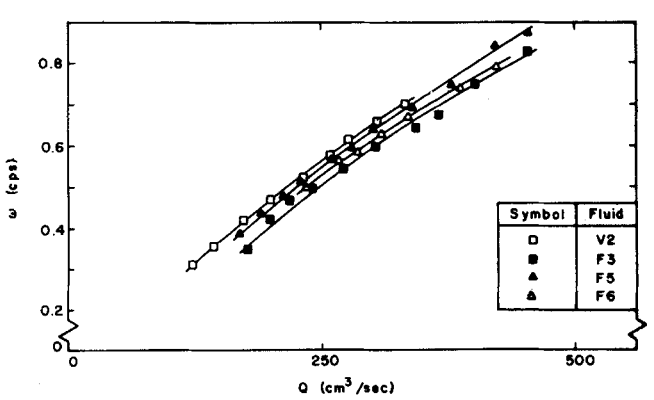

Fig. 2. Frequency of spiralling flow in the 4:1 contraction vs. volumetric flow rate for fluids V2, F3, F5, F6.

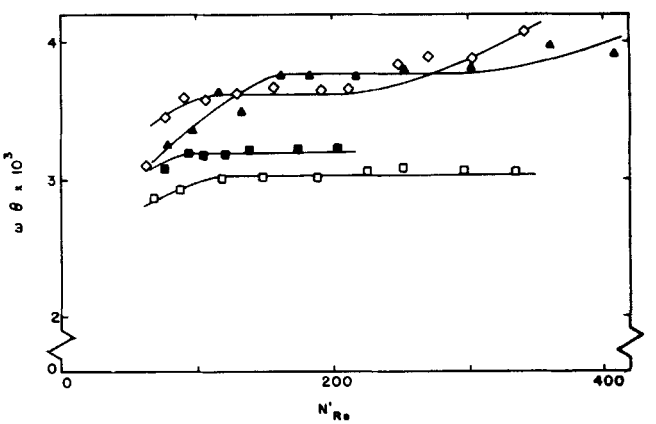

Fig. 3. (Spiralling frequency). (Relaxation time) vs. N_{Re}' for fluids V2, F3, F5, F6 in the 4:1 contraction. Key as in Figure 2.

Fig. 4. Flow pattern upstream of the 4:1 contraction for fluids F14 at 154 cm³/s, showing divergent flow. ($N_{Re}' = 127$, $N_{WS} = 0.483$, 1/5 s at f/8).

into the downstream tube, with symmetrical, cyclic distortions to the converging flow. The upper and lower sections of the vortex seen in Figure 6 collapse and grow with a regular frequency. The distortions to the upper and lower portions of the vortex are in phase. This is distinct from the spiralling flow, where the distortions are in opposite phase.

Consider the spiralling flow pattern of Figure 5, which results from the rotation about the tube center line of an asymmetric distortion to the converging streamlines. Visualize a second distortion added to the flow, similar to the first, but in opposite phase. The second distortion is of equal magnitude to the first and rotates about the tube center line with the same frequency but 180 deg behind. The resultant periodic disturbance to the flow causes the patterns illustrated in Figure 6. This may be interpreted as a double spiral. The double spiral should not be confused with divergent flow. While it is apparent from Figure 6 that the flow pattern is symmetrical on opposite sides of the tube, it continually changes with time. For example, the size of the secondary vortex shown in Figure 6 varies by 50%. Reference must be made to the cine film to fully appreciate the nature of the flow pattern variations with time.

The pulsing distortions described above were only observed with fluids V1, V2, F5, and F14. The common characteristic of these fluids is a relatively low concentration of Separan MG500, less than or equal to 0.6%. In addition, all four fluids were quite fresh. A degraded 0.6% solution (F4) showed neither spiralling nor pulsing flow. It was not possible to identify any distinctly different characteristic of the four fluids from their fundamental viscometric properties.

For the range of flow rates over which multiple steady flow states were obtained, the manner in which the flow was established determined which of the three occurred. If the flow rate was initially low, in the vortex growth regime, and was slowly increased, the resultant entry flow pattern was two-dimensional divergent flow. If the flow rate was increased too rapidly, spiralling flow occurred. Alternatively, the same pattern was obtained if the flow rate was initially high, and the pump speed was slowly reduced. On the other hand, if the pump speed was kept constant, with the pump bypass partially open, and the flow rate through the test section was reduced by partially closing the gate valve downstream of the contraction (refer to Figure 1 in Part I), then it was possible to obtain pulsing flow or a double spiral. The complex manner in which the pulsing flow was obtained complements the extraordinary nature of the entry flow patterns for this condition.

Each of the three flow patterns could be maintained over a period of several hours without any adjustment to valves or pump speeds. This is well beyond the expected life of any transients. Each flow pattern is a true steady state condition. In general, however, the spiralling flow was again the most likely to occur, and the other possibilities may be regarded as metastable.

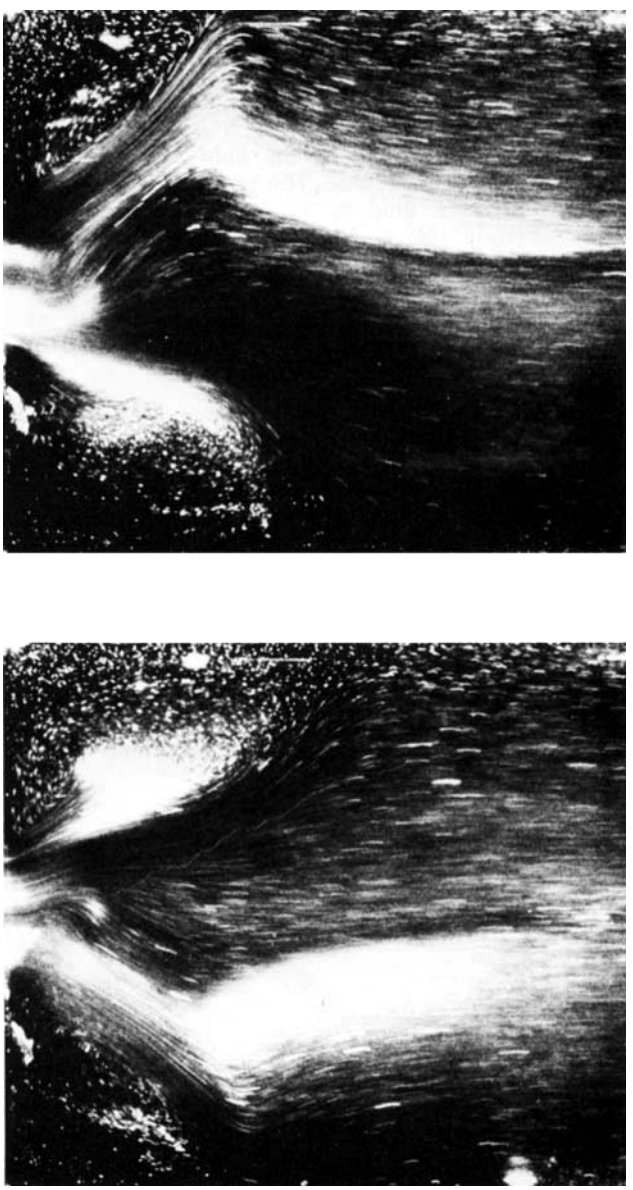

Fig. 5. Flow patterns upstream of the 4:1 contraction for fluid F14 at 154 cm³/s, showing spiralling flow ($N_{Re}' = 127$, $N_{WS} = 0.483$, 1/25 s at f/5.6). (Sequence 1-2 taken short time interval apart.)

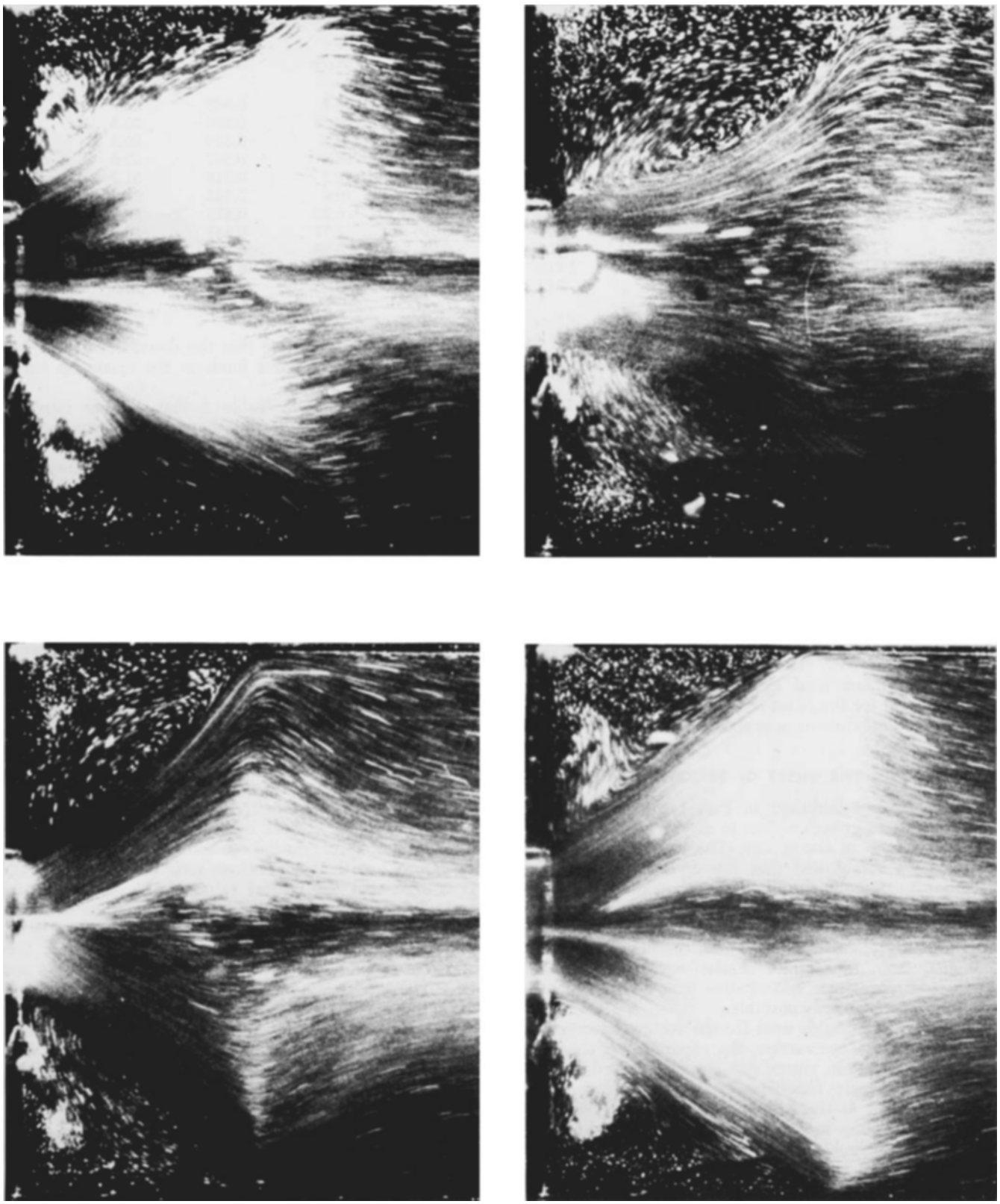

Fig. 6. Flow patterns upstream of the 4:1 contraction for fluid F14 at 154 cm^3/s, showing pulsing flow. ($N_{Re}' = 127$, $N_{WS} = 0.483$, 1/25 s at f/5.6). (Sequence 1-4 taken short time interval apart.)

The development of regular spiralling disturbances in viscoelastic entry region flow has been observed for both polymer melts and solutions by several investigators. For example, Ballenger and White (1971) observed a waving, sinuous motion in the die entry flow of LDPE and polystyrene, which resulted in a helical distortion on the extrudate surface. RamaMurthy (1974) has published comparable results for a viscoelastic polyacrylamide solution and noted that the spiralling frequency increases with shear rate. Den Otter (1970) observed that the frequency of extrudate distortion for a branched PDMS increased significantly with flow rate. Den Otter's results

TABLE 1. EXPERIMENTAL CONDITIONS FOR MAXIMUM VORTEX SIZE FOR ALL FLUIDS TESTED IN THE 4:1 CONTRACTION

Fluid	Q (cm^3/s)	$\dot{\gamma}_w$ (s^{-1})	τ_w (Nt/m^2)	N_{1w} (Nt/m^2)	X_{Max}	N_1/τ	N_{WS}	N'_{Re}	$N_{Re,gen}$
F3	155	790	57.2	754	1.20	13.2	0.565	38.9	129
F4	55.8	251	17.6	93.1	0.57	5.28	0.256	20.3	53.5
F5	93.6	477	26.8	343	1.04	12.8	0.550	30.3	97.0
F6	116	594	38.7	541	1.11	14.0	0.597	32.0	105
F7	132	677	50.3	613	0.94	12.2	0.518	31.7	104
F8	109	537	46.8	470	0.97	10.0	0.445	24.7	79.0
F9	98.3	477	46.1	426	0.89	9.23	0.415	20.9	65.2
F10	87.3	416	43.2	327	0.79	7.57	0.347	18.2	55.0
F11	131	665	75.4	730	0.94	9.68	0.416	21.2	71.0
F12	274	1 440	134	1 618	1.25	12.1	0.504	49.9	174
F13	138	642	63.4	342	0.49	5.40	0.253	32.3	93.4

showed that the frequency varied from 0.02 to 0.8 cycles/s, the same order of magnitude as the results of this investigation shown in Figure 2.

It has already been suggested in Part I that similar mechanisms operate for both polymer melts and solutions in the stable vortex growth regime. It is apparent from the results presented here that the same conclusion applies to the spiralling flow disturbances which can develop once the maximum vortex size condition is passed. In other words, there are unequivocal similarities between polymer melts and solutions in both the stable and unstable flow regimes. These considerations suggest that a criterion for the onset of periodic disturbances to the entry flow of viscoelastic fluids may be obtained from the conditions at which the entry flow characteristics change from those of the vortex growth regime to divergent/spiralling flow. The conditions obtained from the polymer solutions used in these papers are applicable as a criterion for the onset of unstable polymer melt flow, where spiralling disturbances occur.

CRITERIA FOR THE ONSET OF PERIODIC DISTURBANCES

It has been established in Part I that the transition from the vortex growth regime to divergent flow is marked by a maximum in vortex size. The observations outlined above have established that the divergent flow regime is prone to periodic spiralling disturbance. Thus, criteria for the onset of the flow disruption may be based on the experimentally determined conditions for the maximum in vortex detachment length. These conditions are readily obtained from the results of the vortex characteristics study and represent a quantitative limit above which the entry flow is potentially unstable.

For the eleven fluids used for the vortex characteristics study in the 4:1 contraction, the experimental conditions for the maximum in vortex size are summarized in Table 1. All viscometric functions and dimensionless groups were evaluated at the fully developed downstream wall shear rate. Values are given for both the modified and generalized Reynolds numbers. The maximum value of $N_{Re,\,gen}$ is 174, indicating that the downstream tube flow is laminar for all the test fluids at the maximum vortex size condition.

It is apparent from Table 1 that a wide range of critical conditions applies for the onset of disturbed flow for the eleven fluids studied. The critical wall shear stress varies from 18 to 134 Nt/m^2 and the stress ratio from 5.3 to 14. Critical values for N'_{Re} range from 18 to 50 and of N_{WS} from 0.25 to 0.60. Also shown is the maximum value of the dimensionless vortex length, varying from 0.49 to 1.25.

A maximum vortex size condition was also obtained in the 2:1 contraction. Although the flow was not observed to spiral once this condition was exceeded, the divergent flow pattern which was consistently obtained may still be regarded as metastable. The experimental conditions for the maximum vortex size in the 2:1 contraction are summarized in Table 2. These conditions are not as reliable as the data for the 4:1 contraction, owing to the greater uncertainty in the measurement of detachment length. However, it is apparent from Table 2 that the entry flow in the 2:1 contraction becomes potentially unstable at lower flow rates and lower values of N'_{Re} and N_{WS} than in the 4:1 geometry.

The combined critical condition data, specifying the unstable flow condition in both contractions, are presented in Figure 7 as the critical stress ratio (N_1/τ) vs. $N_{Re,\,gen}$. It is seen that the critical value of the stress ratio increases with Reynolds number. A dashed line is drawn through the date indicating approximate proportionality between the stress ratio and the Reynolds number. This apparent proportionality does not apply for fluids F4 and F13. These were the only fluids for which spiralling flow did not occur in the 4:1 contraction. This is possibly due to their significantly lower elasticity levels, or perhaps some other fundamental property which was not measured. This may be an explanation for the significant differences between the critical conditions for these fluids and the remainder.

It would appear from Figure 7 that the critical conditions for the 2:1 and 4:1 contractions all fall on the

TABLE 2. EXPERIMENTAL CONDITIONS FOR MAXIMUM VORTEX SIZE FOR ALL FLUIDS IN THE 2:1 CONTRACTION

Fluid	Q (cm^3/s)	$\dot{\gamma}_w$ (s^{-1})	τ_w (Nt/m^2)	N_{1w} (Nt/m^2)	X_{Max}	N_1/τ	N_{WS}	N'_{Re}	$N_{Re,gen}$
F1	54.3	46.9	20.9	105	0.419	5.03	0.226	1.41	4.40
F2	134	120	41.4	248	0.405	6.00	0.260	4.09	13.5
F3	207	187	34.4	299	0.438	8.69	0.374	11.6	38.5
F4	49.2	38.6	7.38	23.0	0.263	3.11	0.153	3.89	10.2
F5	54.7	49.1	12.0	77.7	0.382	6.48	0.281	2.35	7.52
F6	76.9	69.5	18.2	128	0.415	7.08	0.302	3.02	9.9

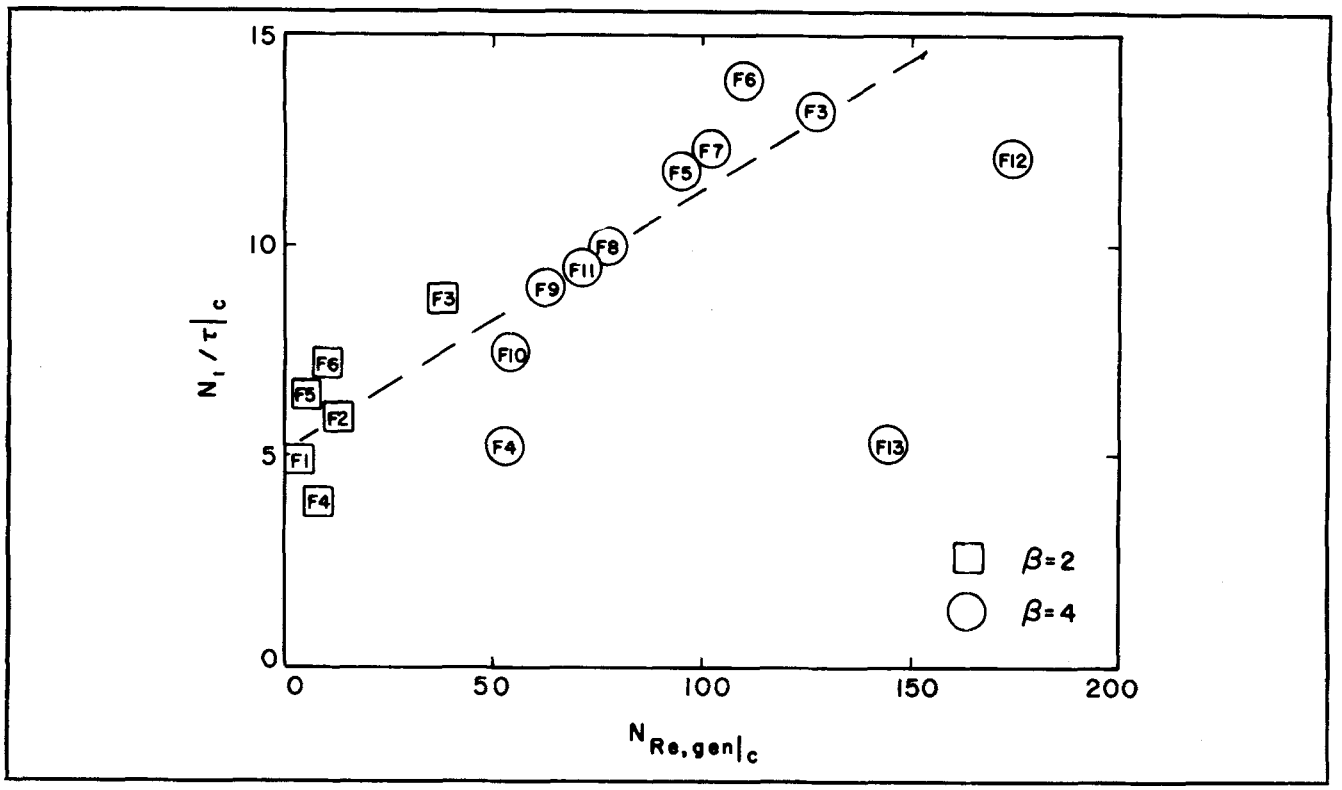

Fig. 7. Critical stress ratio for unstable flow vs. $N_{Re,gen}$ for both geometries.

same straight line, and that the critical stress ratio may be related to the critical Reynolds number as

$$\left.\frac{N_1}{\tau}\right|_c = 5 + 0.07\, N_{Re,\,gen}|_c \qquad (3)$$

This is an experimental criterion for the onset of unstable entry region flow, based on quantitative entry flow pattern observations and fundamental fluid property measurements. Equation (3) gives as a function of Reynolds number the maximum value of stress ratio, in the downstream tube, above which the entry flow will be potentially unstable. It is clear that the effect of fluid inertia is to stabilize the flow, permitting higher levels of fluid elasticity before the flow becomes unstable. The zero Reynolds limit for the stress ratio is 5.

Many criteria have been suggested for the onset of unstable entry region flow. Few have been substantiated by adequate experimental evidence. Boger and Williams (1972) developed a criterion based on equality of a shear wave velocity with a friction velocity. The result was a critical stress ratio of

$$\frac{N_1}{\tau} = \frac{3n+1}{2n} \qquad (4)$$

For the range of power law index for the test fluids in Figure 7, the critical value for stress ratio, calculated from Equation (4), varies from 2.5 to 3.0. Thus, the criterion of Boger and Williams is conservative, based on the experimental creeping flow limit of 5. From a stability analysis of the tube flow of a Maxwell fluid, in creeping flow, Rotherberger et al. (1973) obtained a critical value for the stress ratio of 5.2. The stability analysis was based on axisymmetric perturbations to fully developed tube flow. It is clear from the flow visualization studies that the disturbance to the stable entry flow originates in the entry region and is not axisymmetric. Thus, the apparent agreement between the theoretical result of Rotherberger et al. and the experimental creeping flow limit obtained in this study may be fortuitous.

A careful experimental study by Vlachopoulos and Alam (1972) of melt fracture in polystyrene, based on observations of extrudate distortion, resulted in a correlation of the critical recoverable shear with parameters of the molecular weight distribution. Values for the recoverable shear were estimated using molecular theory. Expressing the result in terms of stress ratio, we obtained the correlation

$$\left.\frac{N_1}{\tau}\right|_c = 5.3\left(\frac{\overline{M}_z\overline{M}_{z+1}}{\overline{M}_w{}^2}\right) \qquad (5)$$

For a monodisperse polystyrene system, the limiting value for the critical stress ratio is 5.3. Again, agreement of this value with the experimental creeping flow limit may be incidental, since the polymers used in this investigation were probably not monodisperse. However, it is interesting to recall that in Part I it was shown that the polymer solutions used in this study represented reasonable models for the behavior of molten polystyrene at higher shear rates, based on consideration of the Maxwellian relaxation time (Figure 5 in Part I).

The various mechanisms which have been proposed for the onset of unstable entry region flow may be considered in the light of the experimental evidence presented in these papers. Applications of hydrodynamic stability analysis have almost exclusively been based on fully developed slit and tube flow. Theoretical predictions of critical condition criteria, using stability analysis, should instead be based on the entry region kinematics described in Part II. In particular, it has been shown that the divergent flow regime is metastable and is prone to assymmetric, spiralling disturbances. These observations may be useful in guiding future theoretical approaches to the hydrodynamic stability problem. The shear wave propagation hypothesis (Coleman and Gurtin, 1968) should be developed by considering propagation into accelerative regions rather than infinite regions undergoing pure shear. In this respect, the kinematic model

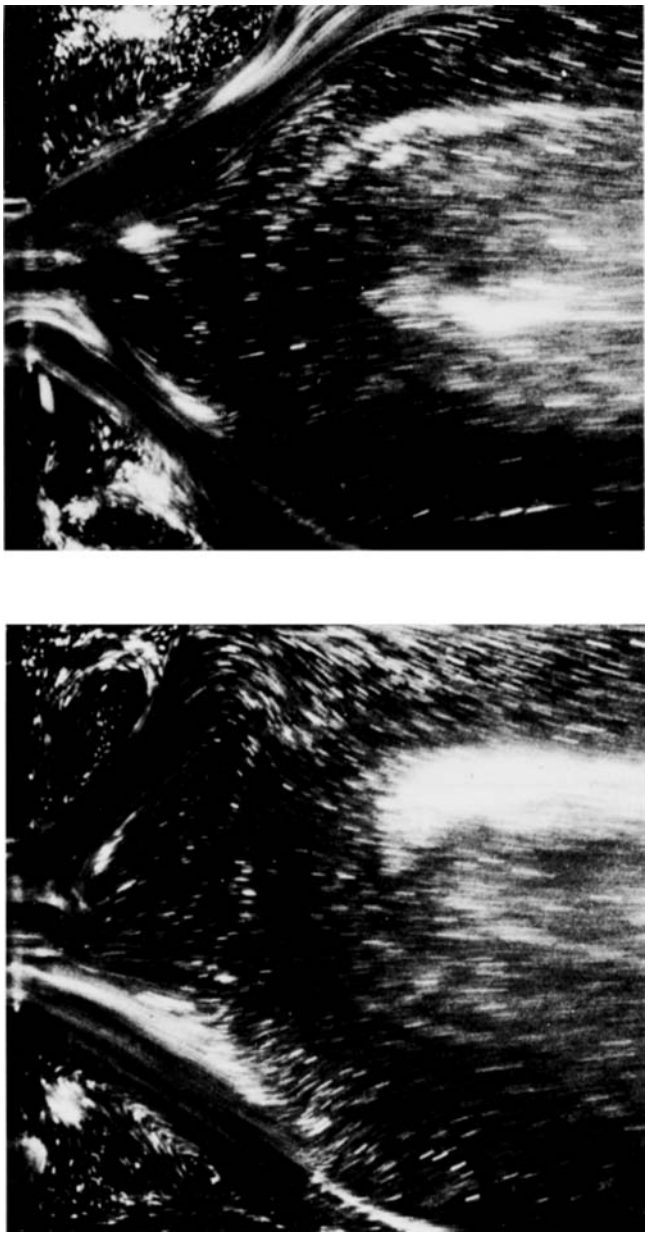

Fig. 8. Flow patterns upstream of the 4:1 contraction for fluid F14 at 550 cm³/s, showing random flow distortions. ($N_{Re'} = 886$, $N_{WS} = 0.829$, 1/100 s at f/2.8.)

proposed for the vortex growth regime may again be applicable.

It has already been shown that extensional strains and stretch rates may be estimated using the kinematic model and steady shear fluid property measurements. Correlation of critical flow conditions in terms of a critical recoverable extensional strain may be seen as equivalent to correlation in terms of steady shear properties. In particular, it has been found that the vortex growth regime is characterized by a constant recoverable extensional strain. This parameter begins to increase once the metastable divergent flow condition is obtained, and periodic flow disturbances become more likely as the extensional strain increases. The use of steady shear measurements in correlating the onset of entry flow disturbances should not be dismissed out of hand. The results of this investigation show that a good correlation is obtained. Future theoretical analysis might be guided by the experimentally defined creeping flow limit and the effect of fluid inertia on the critical conditions. The only variables which merit further experimental investigation are the effect of shear thinning and the die entry angle on the critical conditions for unstable flow.

RANDOM ENTRY FLOW DISTURBANCES

At flow rates higher than those at which the multiple steady flow states occurred, the entry flow patterns became subject to random distortions of a violent nature. An example of the highly disturbed flow is illustrated in Figure 8. Two still photographs are shown of the instantaneous entry flow patterns for fluid F14 in the 4:1 contraction at 550 cm³/s, with $N'_{Re} = 886$ and $N_{WS} = 0.829$. The value for the generalized Reynolds number was 2 400, indicating that the downstream flow was on the edge of the laminar-turbulent transition range. However, flow patterns similar to those shown were observed at lower flow rates, and they must be interpreted as laminar entry flow patterns.

The extreme distortions to the entry flow are evident from the photographs presented. High frequency, non-

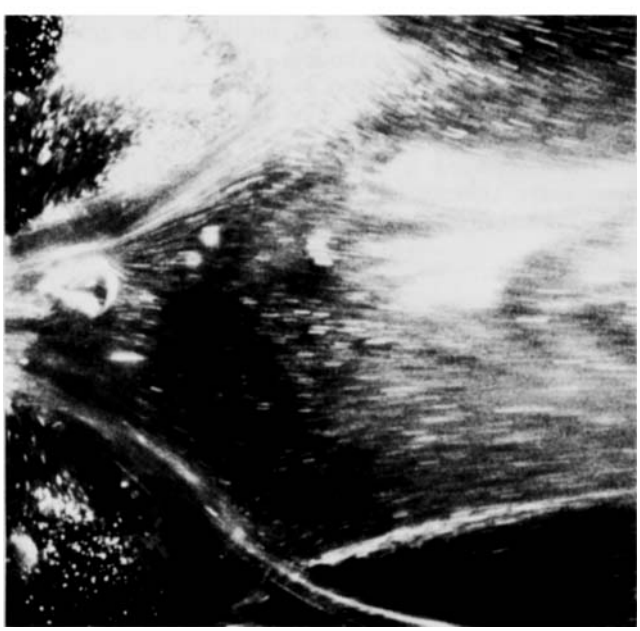

Fig. 9. Flow patterns upstream of the 4:1 contraction for fluid F14 at 550 cm³/s, showing stationary bubble upstream of the small tube entrance. ($N_{Re'} = 886$, $N_{WS} = 0.829$, 1/100 s at f/2.5.)

periodic disturbances to the secondary vortex are accompanied by almost complete stagnation of the flow in the center of the tube. This is shown especially well in Figure 8*a*, where the streak lines in the center of the tube becomes very short just upstream of the small tube entrance, indicating significant fluid deceleration. The majority of the fluid entering the downstream tube is being drawn from the region near the upstream tube wall. This is seen in the photographs as long jets with extremely high velocities. Extended to three dimensions, these jets operate like a pincer, causing the central stagnation zone. The flow patterns are also illustrated on the cine film.

Under the conditions at which the random distortions to the entry flow occurred in the 4:1 contraction, a most unusual phenomenon was observed. It was possible for an air bubble to remain almost stationary in the region just upstream of the small tube entrance for considerable periods. Despite the high average velocity, the bubble would slowly oscillate within the semistagnant central region for some time, prevented from flowing into the downstream tube by the pincerlike action of the high velocity fluid jets entering the small tube from the outer upstream regions. Figure 9 shows two photographs of a stationary bubble in the upstream region, at the same conditions for which the flow patterns in Figure 8 were obtained. The bubble is approximately 5 mm in diameter and was observed to stay in the vicinity of the tube entrance for several minutes before being finally washed downstream. It is clear from the photographs presented that the phenomenon is due to the pincerlike action of the jets of fluid surrounding the stagnant zone. This effect is particularly unusual when it is considered that the average velocity in the downstream tube at the conditions of Figure 9 was 3.4 m/s. This phenomenon is also illustrated on the cine film.

The sudden stopping of large bubbles in an accelerating velocity field for a viscoelastic fluid has been reported previously and was termed the Uebler effect by Metzner (1967). An analysis was presented at the time to explain the phenomenon in terms of the high stresses produced by rapid acceleration and stretching of the fluid. Qualitatively, the effect may be explained by the photographs presented here, which show the pincerlike action of the rapidly deforming fluid jets.

The random distortions to the entry flow which occur at high flow rates represent a separate phenomenon to the multiple steady flow states which prevail at lower flow rates. The entry flow pattern has lost all regularity or periodicity. Criteria for the inception of randomly distorted flow were not obtained because it was not possible to pinpoint the stage at which the regular spiralling flow became haphazard. It is clear that the near stagnant central region just upstream of the small tube entrance is caused by the pincerlike action of the rapidly deforming fluid jets entering the downstream tube. There is some evidence to support the concept of semi solidlike behavior near the sharp corner of the downstream tube entrance. Metzner and Astarita (1967) have described the formation of a solidlike material layer in the vicinity of sharp leading edges in the high Deborah number flow of viscoelastic materials. The sharp corner at the entrance to the downstream tube provides a suitable site for the growth of such solidlike layers. For sufficiently rapid flows, the layer which forms around the circumference of the tube may meet at the center line and cause partial flow stagnation. A more detailed study would be required to substantiate these qualitative remarks.

It is not clear whether the chaotic unstable flow patterns observed for polymer solutions in this study represent parallel behavior to unstable melt entry flow. Certainly, many polymer melts seem to show two stages of instability, spiralling flow being followed by violent distortions at higher flow rates. The violent flow disturbances are characterized by disruption of the central flow lines and surging of material into the downstream conduit from the vortex region, in a pincerlike operation. (Fluid inertial effects tend to be much smaller in melts than solutions, but it is not clear that this is of significance.) Qualitatively, there appear to be some similarities between the two classes of fluid. This is not unexpected, considering the extensive parallels which have been drawn in the stable vortex growth regime and the unsteady spiralling flow condition.

ACKNOWLEDGMENT

The authors are grateful to the Australian Research Grants Commission for their financial support and to the technical staff at the Department of Chemical Engineering at Monash University for their help with all aspects of the experimental work. D. V. Boger is particularly grateful to the Department of Chemical Engineering at the University of Delaware for making possible a very fruitful study leave.

NOTATION

N_1 = First normal stress difference
N'_{Re} = modified Reynolds number
$N_{Re,\,gen}$ = generalized Reynolds number
N_{WS} = Weissenberg number
Q = volumetric flow rate
$\dot{\gamma}$ = shear rate
θ = Maxwell relaxation time
τ = shear stress
ω = frequency of periodic entry flow disturbance

Subscripts

w = conditions at tube wall

LITERATURE CITED

Ballenger, T. F., and J. L. White, "The Development of the Velocity Field in Polymer Melts in a Reservoir Approaching a Capillary Die," *J. Appl. Polymer Sci.*, **15**, 1949-1962 (1971).

Boger, D. V., and H. C. Williams, "Predicting Melt Flow Instability from a Criterion Based on the Behavior of Polymer Solutions," *Polymer Eng. Sci.*, **12**, No. 4, 309-314 (1972).

Coleman, B. D., and M. E. Gurtin, "On the Stability Against Shear Waves of Steady Flows of Non-Linear Viscoelastic Fluids," *J. Fluid Mech.*, 33, No. 1 165-181 (1968).

Metzner, A. B., "Behavior of Suspended Matter in Rapidly Accelerating Viscoelastic Fluids: The Uebler Effect," *AIChE J.*, **13**, No. 2, 316-318 (1967).

———, and G. Astarita, "External Flows of Viscoelastic Materials: Fluid Property Restrictions on the Use of Velocity Sensitive Probes," *ibid.*, No. 3, 550-555 (1967).

Metzner, A. B., and J. C. Reed, "Flow of Non-Newtonian Fluids—Correlation of Laminar, Transition and Turbulent Flow Regions," *ibid.*, **1**, No. 4, 434-440 (1955).

Den Otter, J. L., "Mechanisms of Melt Fracture," *Plastics and Polymers*, 38, 155-168 (1970).

RamaMurthy, A. V., "Flow Instabilities in a Capillary Rheometer for an Elastic Polymer Solution," *Trans. Soc. Rheol.*, **18**, No. 3, 431-452 (1974).

Rothenberger, R., D. H. McCoy, and M. M. Denn, "Flow Instability in Polymer Melt Extrusion," *ibid.*, **17**, No. 2, 259-169 (1973).

Vlachopoulos, J., and M. Alam, "Critical Stress and Recoverable Shear for Polymer Melt Fracture," *Polymer Eng. Sci.*, **12**, No. 3, 184-192 (1972).

Manuscript received April 4, 1977; revision received and accepted March 27, 1978.